ICES Journal of Marine Science

ICES Journal of Marine Science (2021), 78(9), 3265–3280. https://doi.org/10.1093/icesjms/fsab192

Original Article

Explicit incorporation of spatial variability in a biomass dynamics assessment model

Raphaël. R. McDonald [1,2,*], David M. Keith [2], Jessica A. Sameoto[2], Jeffrey A. Hutchings[1,3,4], and Joanna M. Flemming[5]

[1]*Department of Biology, Dalhousie University, 1355 Oxford Street, B3H 1Z2, Canada*
[2]*Population Ecology Division, Fisheries and Oceans Canada, Bedford Institute of Oceanography, PO Box 1006, Dartmouth, NS B2Y 4A2, Canada*
[3]*Institute of Marine Research, Flødevigen Marine Research Station, N-4817 His, Norway*
[4]*Centre for Coastal Research, University of Agder, N-4604 Kristiansand, Norway*
[5]*Department of Mathematics and Statistics, Dalhousie University, Halifax B3H 1Z2, Canada*

[*]*Corresponding author: tel: 1-581-307-7013; e-mail: rp732243@dal.ca*

McDonald, R. R., Keith, D. M., Sameoto, J. A., Hutchings, J. A., and Flemming, J. M. Explicit incorporation of spatial variability in a biomass dynamics assessment model. – ICES Journal of Marine Science, 78: 3265–3280.

Received 17 June 2021; revised 23 August 2021; accepted 12 September 2021; advance access publication 9 October 2021.

The sustainable management of fisheries has largely relied on stock assessment models that assume stocks are homogeneous throughout their domain. However, ignoring complex underlying spatial patterns can lead to increased risk of failures in management. Utilizing geostatistical approaches in conjunction with a traditional fishery biomass dynamics model, we develop a spatially-explicit modelling framework that treats the underlying population dynamics as spatial processes. Simulation experiments demonstrate that this approach reliably estimates variance parameters and accurately captures true patterns of population change. We further demonstrate the utility of our modelling framework in a real setting using data from the Canadian Maritimes Inshore Scallop Fishery. The model captures time-varying spatial patterns in both population characteristics and fishing pressure without explicit knowledge of the underlying mechanisms and retains the ability to scale up to the whole spatial domain with less associated uncertainty than for temporal models. These results lead to improved scientific advice for management, future-proofing of the assessment to shifts in stock productivity and fishing effort, and provide information that can be used to develop more effective management approaches.

Keywords: biomass dynamics model, delay-difference model, *Placopecten magellanicus*, spatial structure, spatio-temporal model, stock assessment.

Introduction

Stock assessment models (SAMs) that often guide the sustainable management of fisheries have traditionally relied on either regression frameworks (Venables and Dichmont, 2004) or fisheries-specific approaches (Hilborn, 1992) to predict changes in fish populations. These methods tend to be strictly temporal in nature and assume that the structure of both the underlying population and the exploitation is homogeneous across space. However, it has long been known that many fisheries exhibit strong spatial patterns in biological characteristics and fishing pressure (Baranov, 1918; Beverton and Holt, 1957; Caddy, 1975; Hutchings, 1996; Smith and Rago, 2004; Smith *et al.*, 2017) that can bias the estimates of population size (Reuchlin-Hugenholtz *et al.*, 2015; Berger *et al.*, 2017; Cadrin, 2020) used to provide advice to fisheries managers (Caddy and Mahon, 1995; Shertzer *et al.*, 2010; Nasmith *et al.*, 2016).

The exclusion of spatial structure in the calculations of population size estimates can result in management failures, which can have serious socioeconomic consequences and long lasting impacts on the conservation of a species. A clear illustration of these

ramifications is evident in the collapse of Atlantic cod (*Gadus morhua*) in Atlantic Canada (Hutchings and Myers, 1994; Myers *et al.*, 1996). The survey indices used at the time did not reflect the ongoing collapse (Hutchings, 1996), whereas recent approaches using spatial methods would have been able to capture the changes in the spatial distribution that heralded the collapse (Reuchlin-Hugenholtz *et al.*, 2016; Carson *et al.*, 2017). More recently, evidence of serial depletion in other fisheries, such as sea cucumbers (Eriksson and Byrne, 2015; Rawson and Hoagland, 2019), indicates that such issues are not relegated to the past. Fortunately, in recent years, various advances have led to the development of statistical methods that can better account for the impact of spatial processes on stock dynamics [e.g. integrated nested Laplace approximation (Illian *et al.*, 2012) and TMB (Kristensen *et al.*, 2016)].

The implementation of more advanced spatial statistic techniques into fisheries research has tended to focus on either generalizations of common regression techniques or geostatistical approaches (Ciannelli *et al.*, 2008). Spatial regression methods focus on modelling the mean, often through generalized additive frameworks (Ciannelli *et al.*, 2008; Pedersen and Berg, 2017). Unfortunately, these methods typically require high-quality information on both environmental variables (temperature, nutrient availability, etc.) and the fish population (scientific surveys, high-quality fisheries data) that are not available for many fisheries (Costello *et al.*, 2012). Alternatively, geostatistical approaches model spatial structure by incorporating spatial autocorrelation into the residual structure of the model (Ciannelli *et al.*, 2008). This has the advantage of capturing the latent spatial variability in the data (Cadigan *et al.*, 2017; Stock *et al.*, 2020) without explicitly modelling the underlying mechanisms. These techniques have been used successfully to improve indices of abundance used for stock assessments (Thorson *et al.*, 2015b; Thorson and Barnett, 2017; Thorson *et al.*, 2019). Focusing on the residual structure allows the mean to be specified using traditional SAMs.

Traditional SAMs, such as biomass dynamics models, often require only an index of population abundance and landings (Hilborn, 1992). They have been extensively used in state-space frameworks (Kinas, 1996; Smith and Hubley, 2014; Best and Punt, 2020) and can be modified to incorporate spatial structure. A significant amount of effort has gone into modelling the spatial autocorrelation in fisheries data to obtain better indices (Thorson *et al.*, 2015b), but comparatively little effort has gone into incorporating the spatial structure in the latent processes of interest such as recruitment (Thorson *et al.*, 2015a). While spatial autocorrelation can be caused by a myriad of factors (Legendre, 1993), unquantified demographic and life-history variability within a stock are likely responsible for a substantial portion of the observed spatial patterns.

Incorporating spatial statistics may benefit many stocks (Berger *et al.*, 2017), particularly sedentary benthic species that have demographic and life-history characteristics that lend themselves more intuitively to spatial modelling. Sea scallops (*Placopecten magellanicus*) are a shellfish species that inhabit the Western North Atlantic from Cape Hatteras to Labrador (Smith and Rago, 2004). These animals exhibit a strong spatial structure in growth rates and reproductive potential, minimal dispersal as adults, and recurring aggregation in scallop beds (Smith and Rago, 2004). Furthermore, the exploitation of these animals tends to focus on areas of high productivity, with fishing effort in these areas being higher than would be expected even if one allocated effort proportionally to the distribution of biomass (Caddy, 1975; Brown *et al.*, 2012; Smith *et al.*, 2017). Explicitly modelling this spatial variability should help improve model predictions and in turn the science advice provided to fisheries managers.

Here we use recently developed statistical advances to incorporate spatial structure into a traditional biomass dynamics model. We modify the strictly temporal state-space model (SSM) described in McDonald *et al.* (2021), referred to as the Tow-Level Model (TLM), to explicitly account for spatial structure; we hereafter refer to this as the Spatially Explicit Biomass Dynamics Assessment Model (SEBDAM). We perform a series of simulations to explore the estimability and identifiability of SEBDAM. We then fit both models (SEBDAM and TLM) to Scallop Production Area 3 (SPA 3) of the Canadian Maritimes Inshore sea scallop fishery as a comparative study.

Methods

Sea scallop data

SPA 3 is a scallop management area in the Bay of Fundy, Canada (Figure 1) managed by Fisheries and Oceans Canada (DFO). This area is managed using total allowable catches in biomass of meat weight (scallop adductor meat). Fisheries assessment advice is derived using a modified version of a delay difference biomass dynamics model (Deriso, 1980; Schnute, 1985; Smith and Lundy, 2002; Smith and Hubley, 2014; Nasmith *et al.*, 2016). The area is surveyed annually using a stratified random sampling design; however, due to the strong spatial structure in the productivity of this stock and spatially aggregated exploitation, the survey design was restratified in 2011 based on the distribution of fishing effort (Smith *et al.*, 2012).

At sea, all live and dead scallops (clappers: dead scallops whose shells are still hinged) are counted and sorted into 5 mm bins. Clappers are used to obtain an estimate of natural mortality. A subset of live scallops (3 per 5 mm bins that are 50 mm and larger) is dissected in order to record individual shell height and meat weight [weight of the adductor muscle (Glass, 2017)]. A length–weight relationship is modelled based on a cube law (Froese, 2006) with depth as a covariate in order to convert all numbers at height to meat weight. Commercial size scallops are defined as having shell heights greater than or equal to 80 mm, and recruits are those between 65 mm and 79 mm, which are expected to grow to be commercial size the following year. We refer to the biomass of recruits as recruitment and to the biomass of commercial size scallops as commercial biomass. The start and end position of each tow are recorded at sea using the commercial vessel navigational system Olex AS (Olex marine survey and navigation, www.olex.no); survey catches are standardized to 800 m length x 5.334 m width.

Model description

SSMs are hierarchical models defined by two stochastic processes: $\mathbf{X}_{s,t}$, $t = 1,\ldots, T$ and $s = 1,\ldots, S$, representing the unobserved dynamic state process describing the real population dynamics between discrete time-steps t and knot locations s, and the observation process $\mathbf{Y}_{s,t}$, which links the observations to the true underlying dynamical processes of interest (Aeberhard *et al.*, 2018). The model parameters are combined in a p-vector $\boldsymbol{\theta} \in \boldsymbol{\Theta} \subseteq \mathbb{R}^p$, and fixed covariates are indicated by $\mathbf{z}_{s,t}$.

$\boldsymbol{\theta}$ is considered a vector of fixed effects and $\mathbf{X}_{1:S,1:T}$ a vector of random effects predicted from estimates of $\boldsymbol{\theta}$. Due to this, the underlying processes (commercial biomass, recruitment, and natural mortality) are considered to be predicted in years with data, with future predictions in years without data referred to as projections. These projections are obtained by moving the process equations

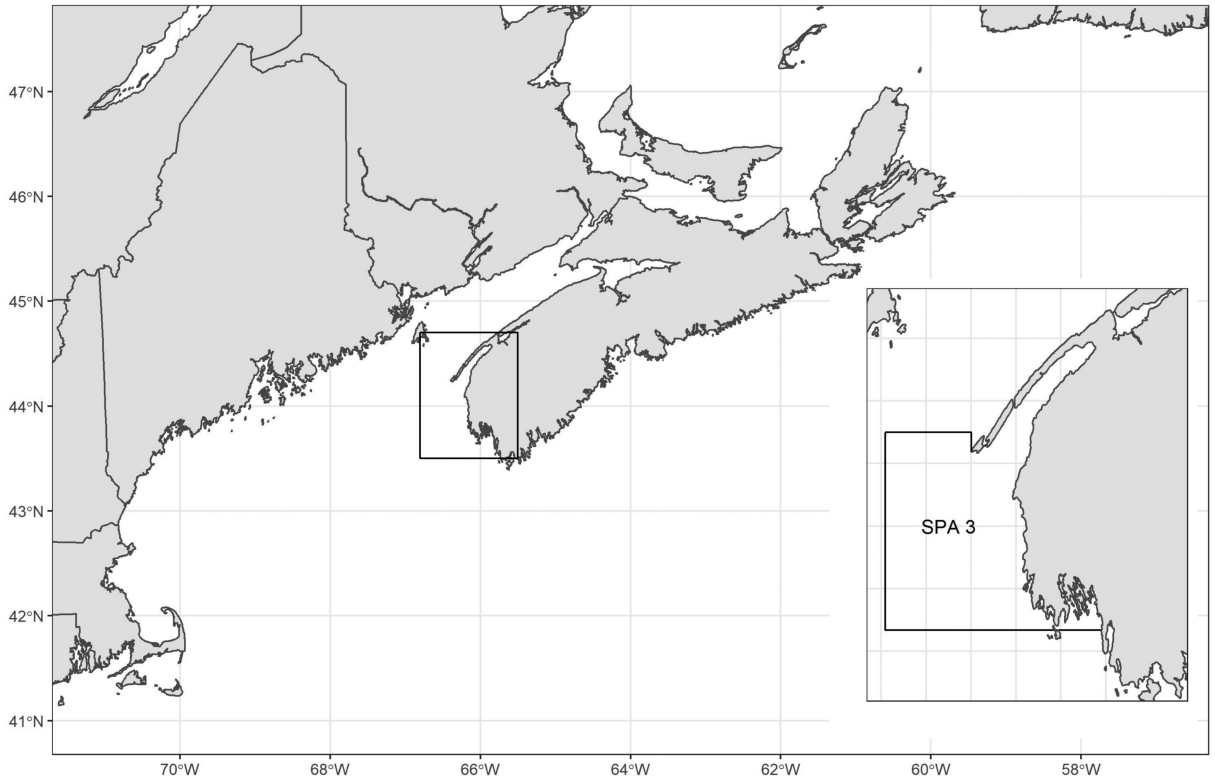

Figure 1. Newfoundland to Cape Cod with inset map of SPA 3 off South West Nova Scotia, Canada.

forward 1 year and therefore represent the predicted mean and uncertainty. This is meant as an illustration of potential uncertainties when predicting in years without data. These variables can be combined into the following joint likelihood $L(\cdot)$ and marginal log-likelihood $\mathcal{L}(\cdot)$:

$$L(\boldsymbol{\theta}, \mathbf{Y}_{1:T}, \mathbf{X}_{1:T}) = \prod_{s=1}^{S} p(\mathbf{Y}_{s,1}|\mathbf{X}_{s,1}, \boldsymbol{\theta}) \prod_{t=2}^{T} p(\mathbf{Y}_{s,t}|\mathbf{X}_{s,t}, \boldsymbol{\theta}) \times p(\mathbf{X}_{s,t}|\mathbf{X}_{s,t-1}, \boldsymbol{\theta}), \quad (1)$$

$$\mathcal{L}(\boldsymbol{\theta}, \mathbf{Y}_{1:S,1:T}) = log \int L(\boldsymbol{\theta}, \mathbf{Y}_{1:S,1:T}, \mathbf{X}_{1:S,1:T}) d\mathbf{X}_{1:S,1:T}. \quad (2)$$

Approximations for these high-dimensional integrals are obtained using the Laplace method as implemented in the TMB package in R (Kristensen *et al.*, 2016). TMB's use of automatic differentiation has been shown to be computationally more efficient than most other packages without loss of accuracy (Kristensen *et al.*, 2016; Auger-Méthé *et al.*, 2017).

Spatial approach

The predictive framework described in Thorson *et al.* (2015b) is adopted here. Instead of modelling a given random field over every possible location, its value is approximated as being piece-wise constant. The user must specify the number of locations, called "knots", at which the model will track the value of the random field. This choice drives both the resolution of the model predictions and the computational load, since more knots leads to higher resolution but the fitting process will be slower. The decision concerning the number of knots used should be based on the spatial coverage of the data to control the accuracy of the piece-wise approximation. The locations of these knots are obtained by applying a k-means clustering algorithm on the location of all the survey tows. The number and location of knots is held constant for model fitting and all observations (both survey tows and landings) are attributed to the closest knot. In summary, the locations of the tows are used to obtain the knots, which are then used to create the mesh and are the only vertices inside that mesh that have data, as each tow is attributed to its closest knot. This allows the knots to have multiple replicate observations of the underlying processes in any given year.

Preliminary tests were undertaken with different numbers of knots to determine the optimal resolution. We chose to use 25 knots to strike a balance between computational demand and performance. The north-west section of SPA 3 is known to contain very few scallops due to the benthic substrate being primarily glaciomarine mud (Shaw *et al.*, 2012, 2014) and it is therefore not regularly included in the DFO survey domain; as such it was removed from the modelled area. The resulting grid is shown in Figure 2 alongside the triangulation used for model predictions.

Spatially explicit biomass dynamics assessment model

A previous model, the TLM, tested the impact of directly incorporating tow level data into a SAM without first aggregating them into indices (McDonald *et al.*, 2021). This TLM is highly similar to SEBDAM, except that the spatial components are absent. Spatial information is incorporated into SEBDAM through the use of Gaussian Markov Random Fields (GMRFs), using the Stochastic Partial Differential Equation (SPDE) approach with a Matérn covariance structure (Lindgren and Rue, 2011). Only two parameters are required for this approach: κ, which is related to range ρ ($\rho = \sqrt{8}/\kappa$) and controls the distance at which two points become uncorrelated,

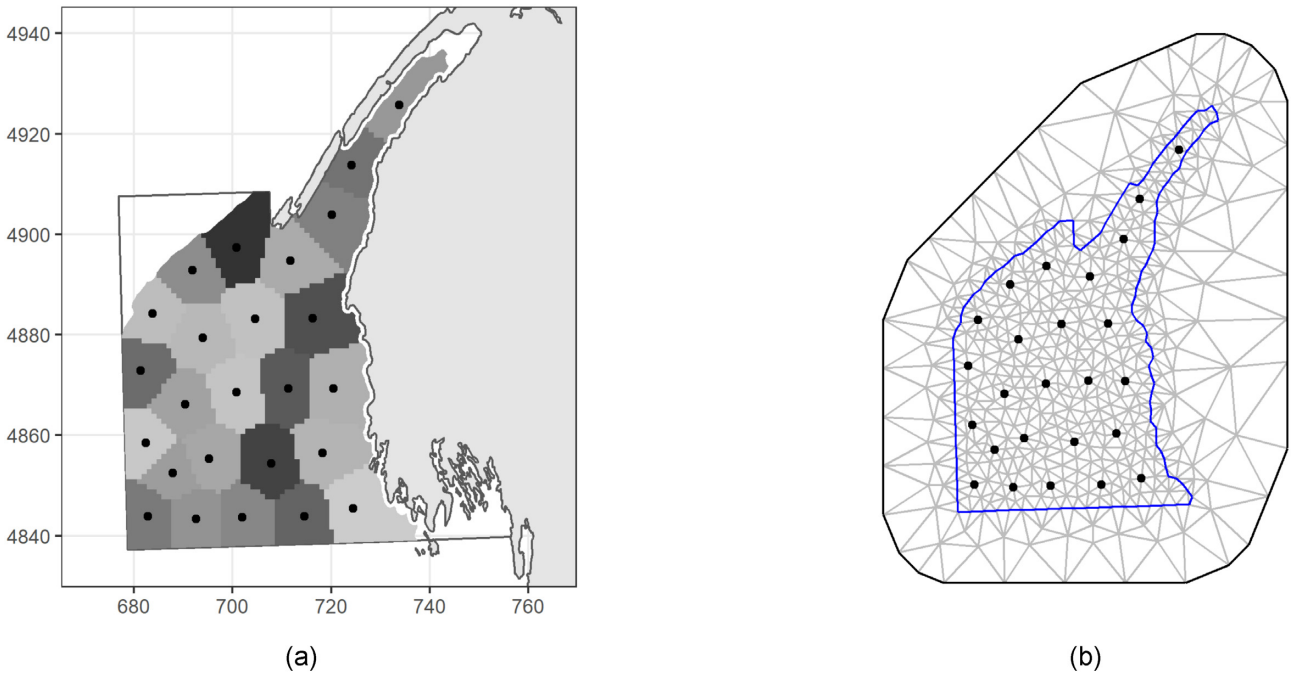

Figure 2. a: Grid used to analyze SPA 3 with knots shown as black points and black lines indicating the management boundary for the area (greyscale used for visualization purposes). Nearshore knots are the nine easternmost knots, with the other knots considered offshore knots. b: Delaunay triangulation used for the model with black points indicating location of each knot.

and τ, which controls the spatial variance [for details see Lindgren and Rue (2011) and Lindgren (2012)].

The locations of the observations are projected onto the Universal Transverse Mercator (UTM) system so that the spatial parameters are more interpretable since UTM coordinates are in meters (rescaled into kilometers for numerical stability).

Using the SSM hierarchical framework, we model the underlying process dynamics with the following equations:

$$B_{s,t} = [exp(-m_{s,t})g_{t-1}(B_{s,t-1} - C_{s,t-1}) + exp(-m_{s,t})g^R_{t-1}R_{s,t-1}]exp\left(\Omega^B_{s,t}\right), \quad (3)$$

$$R_{s,t} = R_{s,t-1}exp\left(\Omega^R_{s,t}\right), \quad (4)$$

$$m_{s,t} = m_{s,t-1}exp\left(\Omega^m_{s,t}\right). \quad (5)$$

Equation (3) is the simplified delay-difference equation where $B_{s,t}$ are the commercial biomass densities, $C_{s,t}$ are landings, $R_{s,t}$ are the recruitment biomass densities, $m_{s,t}$ are the instantaneous natural mortalities, and g_t and g^R_t are the commercial size and recruit growth rates, respectively, which are estimated separately (Smith and Hubley, 2014; Nasmith *et al.*, 2016). $\mathbf{\Omega}^B_t$ is the GMRF for commercial biomass in year t, which, using the SPDE approach, is reduced to a mean zero multivariate normal where its covariance matrix is $\mathbf{\Sigma}(s, s') = Matérn(||\mathbf{H}^B(s - s')||)$, indicating that the covariance between two knots s and s' where $s \neq s'$ follows a Matérn covariance structure. This structure allows for geometric anisotropy through $\mathbf{H}^B$, which is defined to maintain volume and has two parameters [for more details see Thorson *et al.* (2015b)]. The value at each knot s for year $t = 1$ is simply $B_{s,1} = B_0 * exp(\Omega_{s,1})$ where B_0 is an estimated mean parameter.

Equations (4) and (5) are lognormal random walks where the error terms $\mathbf{\Omega}^R_t$ (recruitment) and $\mathbf{\Omega}^m_t$ (natural mortality) are GMRFs that are parameterized by the same methods as Equation (3). Recruitment is assumed to have the same anisotropy matrix as the commercial biomass, while natural mortality has a separate matrix. The value at each knot s for year $t = 1$ are $R_0 * exp(\Omega^R_{s,1})$ and $m_0 * exp(\Omega^m_{s,1})$ where R_0 and m_0 are estimated mean parameters. The commercial biomass and recruitment for the whole area, hereafter referred to as the total biomass and recruitment, can be derived

Table 1. Parameters used and their optimization starting values.

Parameter	Simulation value	Optimization starting value
κ_B	0.071	exp(-1)
τ_B	19.947	exp(1)
κ_R	0.047	0
τ_R	29.921	0
κ_m	0.141	0
τ_m	19.947	0
σ_ϵ	0.500	exp(-1)
σ_υ	0.500	exp(-1)
S	0.600	exp(-1)
R_0	100.000	150
B_0	600.000	3000
m_0	0.300	exp(-1)
q_R	0.200	exp(-1)
p_I	0.950	0.5
p^R_I	0.500	0.5
H^{B1}_{input}	− 1.200	0
H^{B2}_{input}	− 0.500	0
H^{m1}_{input}	− 0.500	0
H^{m2}_{input}	0.400	0

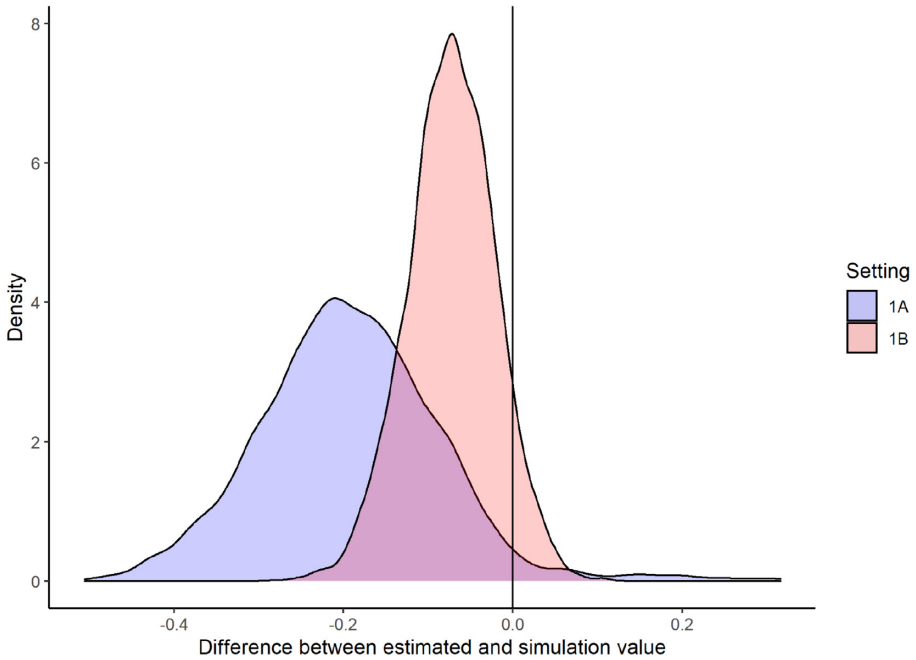

Figure 3. Density plot of the differences between estimated $q_{I(s)}$ and simulation value for settings 1A (blue) and 1B (red). Black vertical line indicates zero difference.

by multiplying $B_{s,t}$ and $R_{s,t}$ by the area covered by their respective knots, then summing up over all knots s.

The observations are linked to the underlying processes through the following equations:

$$I_{i,s,t} = \frac{q_{I(s)}B_{s,t}}{p_I}\epsilon_{i,s,t}, \quad \epsilon_{i,s,t} \overset{Ind}{\sim} u\ell N\left(\sigma_\epsilon^2\right), \tag{6}$$

$$I^R_{i,s,t} = \frac{q_R R_{s,t}}{p^R_I}\upsilon_{i,s,t}, \quad \upsilon_{i,s,t} \overset{Ind}{\sim} u\ell N\left(\sigma_\upsilon^2\right), \tag{7}$$

$$L_{i,s,t} \overset{Ind}{\sim} Bin\left(n_{i,s,t}, m_{s,t}S\right). \tag{8}$$

Equation (6) links the observed survey commercial biomass $I_{i,s,t}$ in tow i at knot s and year t to the underlying biomass density $B_{s,t}$ scaled by the commercial size catchabilities $q_{I(s)}$ at each knot and adjusted by the probability of positive tows p_I. In comparison to usual approaches where there would be a unique catchability parameter for the whole area, it was decided to let the commercial size catchability vary through space. This is due to this area being known to have variable bottom types (Greenlaw *et al.*, 2010), which is known to impact gear efficency (Miller *et al.*, 2019). Following the delta approach, p_I is estimated separately (with uncertainty propagated forward) through a binomial distribution based on the number of zeroes and non-zero survey tows.

Equation (7) is conceptually identical with the recruitment equivalent to Equation (6), with observed survey recruit biomass $I^R_{i,s,t}$, underlying recruitment density $R_{s,t}$, a single non-spatial recruit catchability q_R, and probability of positive recruit catches p^R_I, which is also estimated through a binomial distribution based on the number of survey tows with positive recruit catches.

Equation (8) links the number of clappers $L_{i,s,t}$ to the natural mortality $m_{s,t}$ scaled by clapper catchability S through a binomial distribution based on the number of commercial size paired shells (both clappers and live scallops) $n_{i,s,t}$ caught in tow i at knot s in year t.

In summary, SEBDAM contains the observed states $\mathbf{Y}_{s,t} = (I_{i,s,t}, I^R_{i,s,t}, L_{i,s,t})^T$, the unobserved states $\mathbf{X}_{s,t} = (B_{s,t}, R_{s,t}, m_{s,t})^T$, the fixed covariates $\mathbf{z}_{s,t} = (n_{i,s,t}, C_{s,t}, g_t, g^R_t)^T$, and the parameters $\boldsymbol{\theta} = (p_I, p^R_I, q_{I(s)}, q_R, S, \sigma^2_\epsilon, \sigma^2_\upsilon, B_0, R_0, m_0, \tau_B, \tau_R, \tau_m, \kappa_B, \kappa_R, \kappa_m, \mathbf{H}^B_{input}, \mathbf{H}^m_{input})^T$.

Simulation study

This simulation study aims to assess the identifiability and estimability of SEBDAM and consists of two different settings both using the same simulation design. Setting 1A does not inform the estimation of $q_{I(s)}$, while 1B informs the estimation of $q_{I(s)}$ using a beta distribution with shape parameters $\alpha = 10$ and $\beta = 12$ [slightly modified from the prior distribution used in DFO assessments; see Yin *et al.* (2019) for details]. A secondary study that examines the impact of fitting a strictly temporal model to data with spatial structure is described in Appendix A.

The simulation area is a 50 km by 50 km square. Data for 20 years with 125 tows each year are simulated to mimic a similar size to the SPA 3 dataset. The locations of these 2500 data points are randomly assigned across the simulation area from which knots are then obtained. g_t and g^R_t are assumed constant and set at 1.1 and 1.5, respectively, to reflect the average growth rates seen in the SPA 3 data. The total number of live and dead scallops caught ($n_{i,s,t}$) is set to 120 in every tow.

The parameter values chosen for the simulations along with the starting values used during optimization are shown in Table 1 except for the 25 $q_{I(s)}$, whose optimization starting values are all $exp(-1)$. The parameters for $\mathbf{H}^B_{input}$ are chosen to simulate strong anisotropy where the decorrelation range north-south is much larger than east-west, while those for $\mathbf{H}^m_{input}$ are made to decorrelate rapidly in all directions. Range parameters κ_B, κ_R, and κ_m were obtained by setting mean decorrelation ranges of the GMRFs at 40 km for the commercial biomass, 60 km for recruitment, and 20

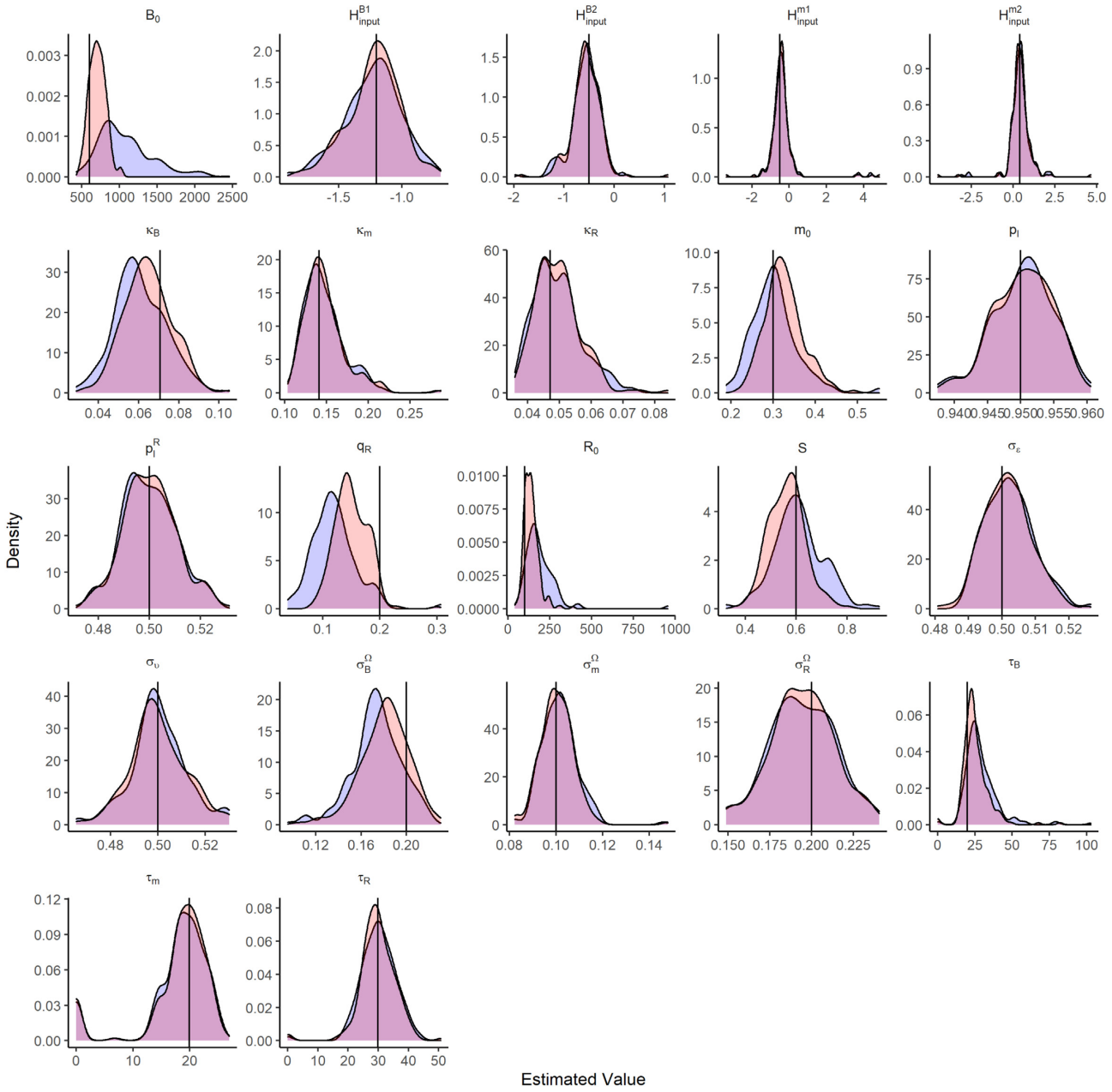

Figure 4. Density plots of parameter estimates from setting 1A (blue) and 1B (red). Black vertical line is simulation value.

km for mortality. Following the relationships between the marginal variance and parameters estimated through the SPDE approach (Lindgren, 2012), the spatial variability parameters τ_B, τ_R, and τ_m are obtained by setting the marginal variance of the random fields at 0.2 for $\boldsymbol{\Omega}_t^B$ and $\boldsymbol{\Omega}_t^R$ and 0.1 for $\boldsymbol{\Omega}_t^m$.

While the landings are not explicitly modelled by SEBDAM, we aim to mimic realistic settings where fisheries tend to exploit areas of higher biomass (Smith *et al.*, 2017). The total exploitation in each year is simulated from a lognormal distribution with a mean set to 10% of the simulated total biomass and a variance of 0.2 on the log scale. This total exploitation is then divided proportionally between knots with higher than average biomass following another lognormal distribution with a variance of 0.2 on the log scale. This results in approximately half the knots being fished extensively, while knots with lower biomass densities are not fished at all. Scripts for running the simulations are available at https://github.com/RaphMcDo/SPA3-Case-Study.

Application to the Bay of Fundy sea scallop fishery

This application explores how SEBDAM performs when fit to real fishery data, using the SPA 3 scallop population. Its performance is compared to TLM. Our primary goal is to compare model performance to examine the effects of incorporating spatial structure. We also examine the effects of estimating multiple spatial catchabilities in SEBDAM (TLM assumes a single catchability parameter).

While survey data are available from 1996 to 2018, detailed logbooks are only available from 1998 to 2018. The stock dynamics are

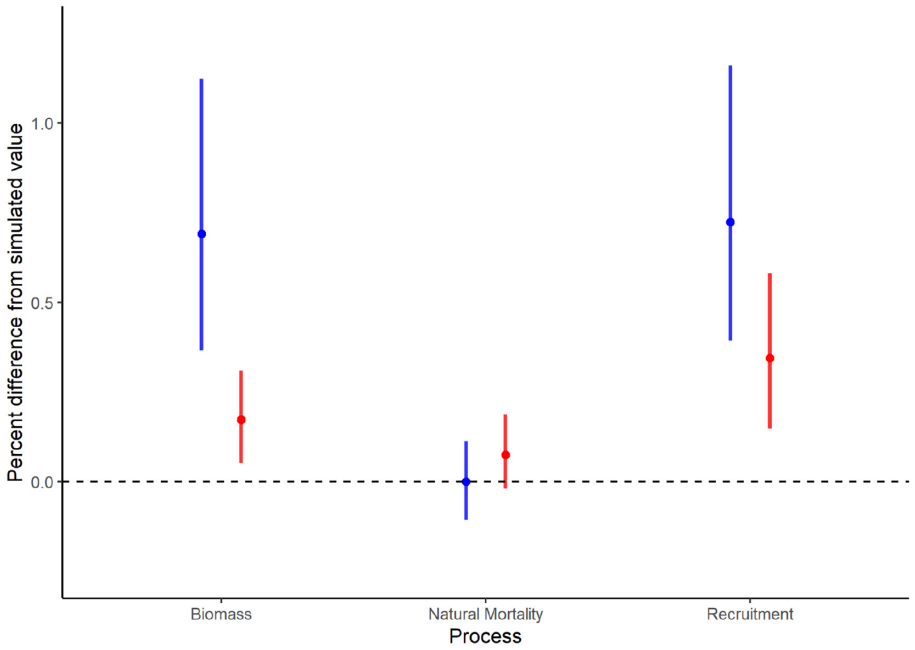

Figure 5. Median and interquartile range of the differences between predicted processes and their simulated value for settings 1A (blue) and 1B (red).

Table 2. Parameter estimates and standard errors for SEBDAM and TLM after being fitted to SPA 3 with q_I and $q_{I(s)}$ informed with a beta distribution.

SEBDAM			TLM		
Parameter	**Estimate**	**SE**	**Parameter**	**Estimate**	**SE**
κ_B	0.047	0.013	σ_τ	0.168	0.041
τ_B	24.347	7.639	σ_ϕ	0.278	0.070
κ_R	0.060	0.011	σ_η	0.533	0.078
τ_R	15.434	3.451	σ_ϵ	1.165	0.016
κ_m	0.181	0.021	σ_υ	1.071	0.024
τ_m	1.541	0.165	q_I	0.422	0.109
σ_ϵ	1.017	0.014	q_R	0.071	0.054
σ_υ	0.919	0.021	S	0.277	0.143
S	0.572	0.080	p_I	0.917	0.005
R_0	93.108	35.266	p_I^R	0.350	0.009
B_0	467.500	112.113			
m_0	0.059	0.022			
q_R	0.052	0.016			
p_I	0.918	0.005			
p_I^R	0.350	0.009			
H_{input}^{B1}	− 1.056	0.324			
H_{input}^{B2}	− 0.856	0.445			
H_{input}^{m1}	0.031	0.321			
H_{input}^{m2}	− 0.161	0.259			

therefore modeled from 1997 to 2018 utilizing a total of 3035 survey tows, with a 1-year ahead projection for 2019. This one-year projection utilizes the same model and calculates the projection based on the estimated parameters and predicted random effects while propagating errors forward. Both models are fitted using the TMB package in R and the *nlminb* optimizer. Optimization starting values are in Table 1. Preliminary analyses indicate that the model is somewhat sensitive to the values of κ_B and τ_B, which is why their optimization starting values are different than the spatial parameters for the other processes. Random effects starting values are set to 0 for all random fields. Previous work has shown clear improvements in biomass predictions when informing q_I for TLM (McDonald *et al.*, 2021) and preliminary analyses indicates similar improvements for SEBDAM. Therefore, both SEBDAM and TLM are fitted to SPA 3 data twice, once without informing q_I and $q_{I(s)}$ and once informing them using a beta distribution. While both models utilize different statistical methodologies, which can be difficult to compare (Aubry and Debouzie, 2000), both models try to predict the true realization of the stochastic process for biomass. As there is only one dataset, and therefore one realization of this process, the main interest is to examine how both models treat the data to obtain an estimate of this actual realization. Survey data and R script are available at https://github.com/RaphMcDo/SPA3-Case-Study.

Results

Simulation results

For all simulation settings, the majority of simulations converged. For setting 1A, 191 simulations converged, two resulted in false convergence, six resulted in singular convergence, and one did not converge. For setting 1B, 197 simulations converged, two resulted in singular convergence and one did not converge. The catchabilities ($q_{I(s)}$ in Figure 3, q_R and S in Figure 4) are underestimated for both settings but this bias is smaller when $q_{I(s)}$ are informed (setting 1B). Informing $q_{I(s)}$ reduces the consistent bias in commercial size catchabilities with the mean percent difference going from −48% to −18% (Figure 3). While the biomass and recruit processes are positively biased, the reduced estimation bias of $q_{I(s)}$ further leads

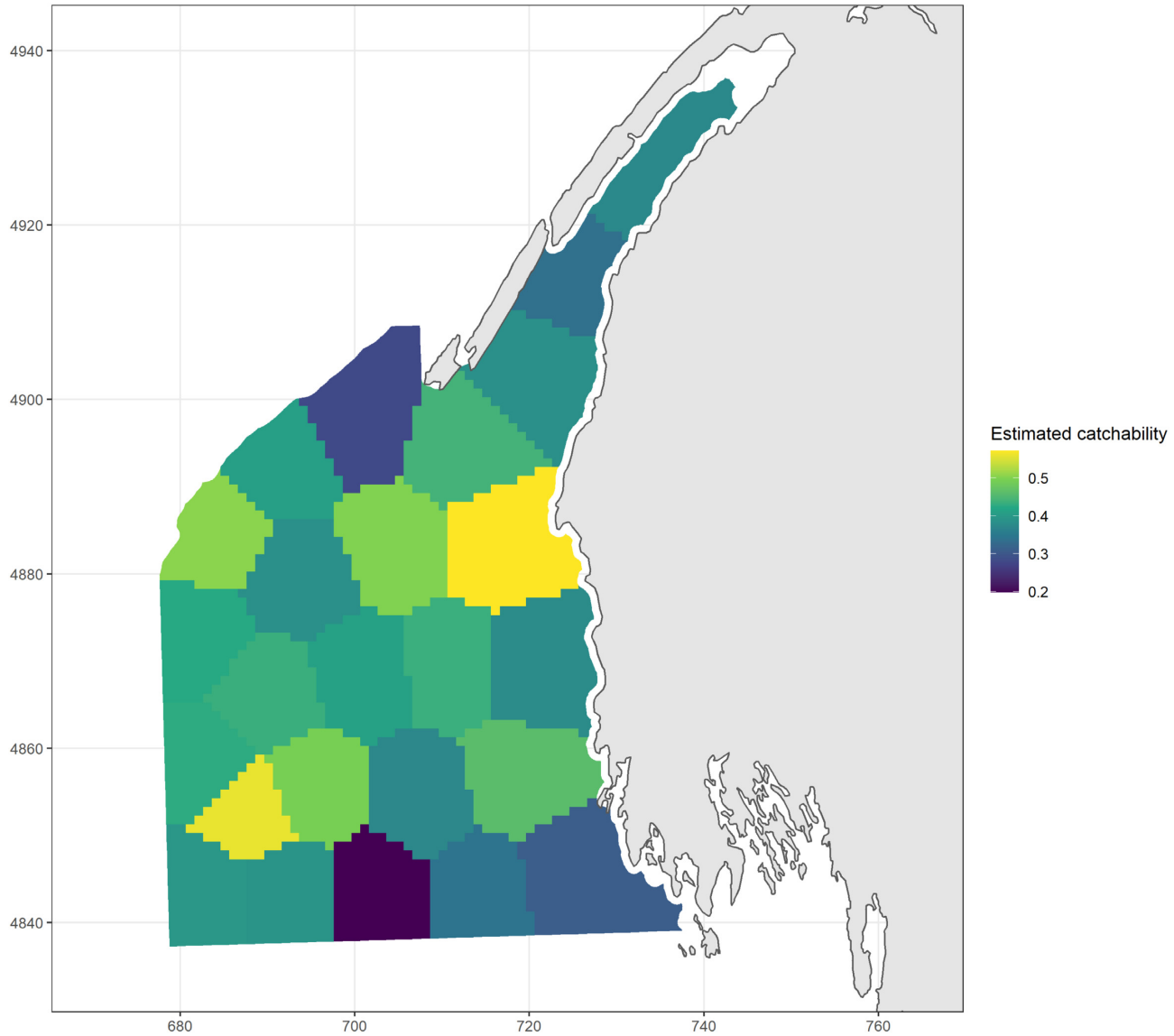

Figure 6. Estimated commercial size catchabilities by SEBDAM at each knot in SPA 3 when informed with beta distribution.

to a comparable reduction of this bias in predicted biomass and recruitment (Figure 5). However, this does not impact the prediction of natural mortality substantively (Figure 5).

The distribution of estimated spatial parameters (κ, τ, and H_{input}) are centered near the value used for simulations for both settings, e.g. 70% of estimates for κ_B are within 25% of simulation value in 1A (Figure 4). The GMRF marginal variances (σ_B^{Ω}, σ_R^{Ω}, and σ_m^{Ω}) are well captured, e.g. 83% of estimates are within 25% of simulation value for σ_B^{Ω} for 1A (Figure 4).

Application to scallop data

The simulations in 1A and 1B demonstrated that the outputs were more reliable when the $q_{I(s)}$ were informed. Thus, we focus on the output from the model fits where the commercial size catchabilities are informed (see Supplementary Materials for output when uninformed). Both models converged successfully with parameter estimates shown in Table 2 and Figure 6. SEBDAM identifies fine-scale time-varying spatial patterns of commercial biomass (Figure 7). Parameter estimates and standard errors for SEBDAM fit to the SPA 3 data with a single commercial size catchability parameter q_I are available in the Supplementary Materials.

The nearshore areas tend to have increased biomass in later years (e.g. 21.9% of total biomass between 2012 and 2018 in nine knots compared to 17% between 1997 and 2004 in the same knots). The knots with the highest predicted density are also the areas under higher fishing pressure (the nine nearshore knots contain 91.1% of the total effort between 2012 and 2018) and correspond to the majority of the area currently included in the stock assessment (Nasmith *et al.*, 2016).

Time-varying spatial patterns of recruitment and natural mortality are also identified by the model (Figures 8 and 9). The outer areas tend to have consistently higher natural mortality rates than the rest of SPA 3 (average of 0.12 for the 16 outer knots). Recruitment is less spatially consistent, it tends to be higher in the nearshore areas in later years (e.g. 40.9% of recruitment between 1997 and

Figure 7. Predicted commercial biomass density $B_{s,t}$ (kg/km^2) at each knot between 1997 and 2018, with 1-year projections for 2019.

2006 in the nine nearshore knots and 64% between 2012 and 2018).

The marginal variances of the Matérn covariance structures [calculated following relation in Lindgren (2012)] are 0.29 for $\mathbf{\Omega}^B$, 0.35 for $\mathbf{\Omega}^R$, and 1.05 for $\mathbf{\Omega}^m$ when $q_{I(s)}$ are uninformed. When they are informed the marginal variances are 0.21 for $\mathbf{\Omega}^B$, 0.45 for $\mathbf{\Omega}^R$, and 1.01 for $\mathbf{\Omega}^m$.

The natural mortality, while it decorrelates relatively rapidly in all directions (mean decorrelation range of 14.8 km, Figure 10), is still highest in the areas closest to the glaciomarine mud bottom (Shaw *et al.*, 2014). Both commercial biomass and recruitment decorrelate rapidly on the east-west axis, but stay correlated at large distances on the north-south axis (mean decorrelation ranges of 40.9 km and 39.1 km, respectively, Figure 10).

Aggregating over the whole area, TLM predicts higher total commercial biomass than SEBDAM, with the difference narrowing over time (Figure 11). The difference was on average 15.5% from 1997 to 2003 and declined to an average difference of 9.1% between 2013 and 2018 (the average difference was 9.6%). The convergence in the biomass predictions between TLM and SEBDAM in more recent years mirrors the results from the secondary simulation experiment (see Appendix A). The 95% confidence interval of the SEBDAM biomass predictions are 65.7% smaller than for TLM. The uncertainty of the 1-year projection (2019) was more similar between

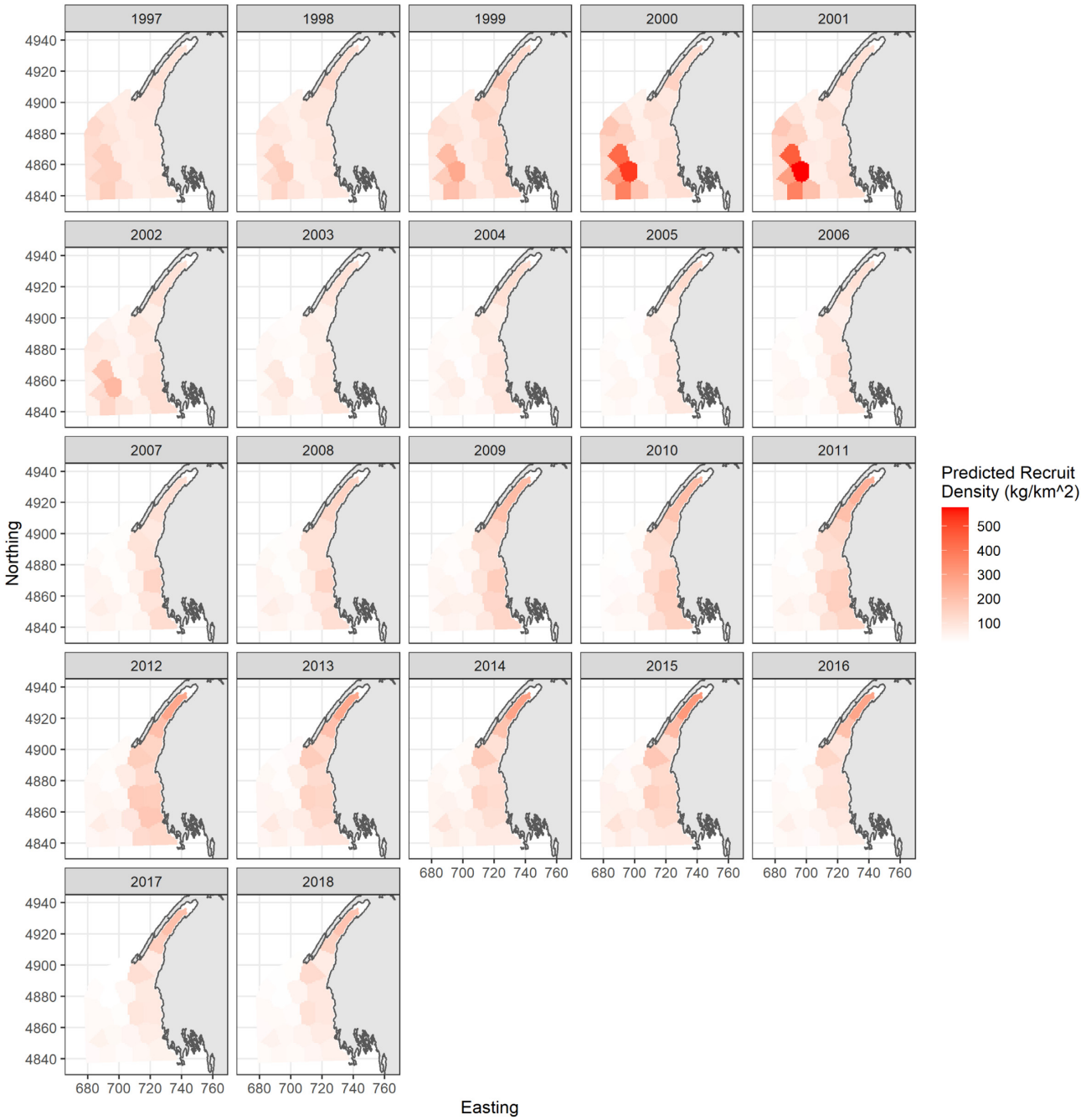

Figure 8. Predicted recruit biomass density $R_{s,t}$ (kg/km^2) at each knot between 1997 and 2018.

the two models as the 95% confidence interval from SEBDAM was 33.8% smaller than for TLM. The recruitment predictions of SEBDAM and TLM are very similar, but the 95% confidence interval for TLM are on average 126.3% larger than for SEBDAM.

The mean natural mortality predicted by SEBDAM is on average lower by 0.09 than the one predicted by TLM. The effects of particularly strong influential tows with a high proportion of clappers is greatly reduced for SEBDAM, which is clearly seen in 2003 (Figure 11). While these tows inform localized mortality patterns (e.g. the elevated mortality in the outside area; Figure 9), they are no longer extrapolated to the entire population in SEBDAM (Figure 11, see Figure 14 in Supplementary Materials for visualization of individual tows in 2003). The reduced impact of strong influential tows is also present for biomass and recruitment, but is most evident for the natural mortality. This also results in substantially smaller 95% confidence intervals for natural mortality in SEBDAM, which are 136.5% smaller on average than for TLM.

Discussion

SEBDAM reliably captures population changes across both space and time while simultaneously accounting for spatio-temporal patterns in productivity. Furthermore, it has the relatively uncommon ability to incorporate spatio-temporal patterns in exploitation (Cao

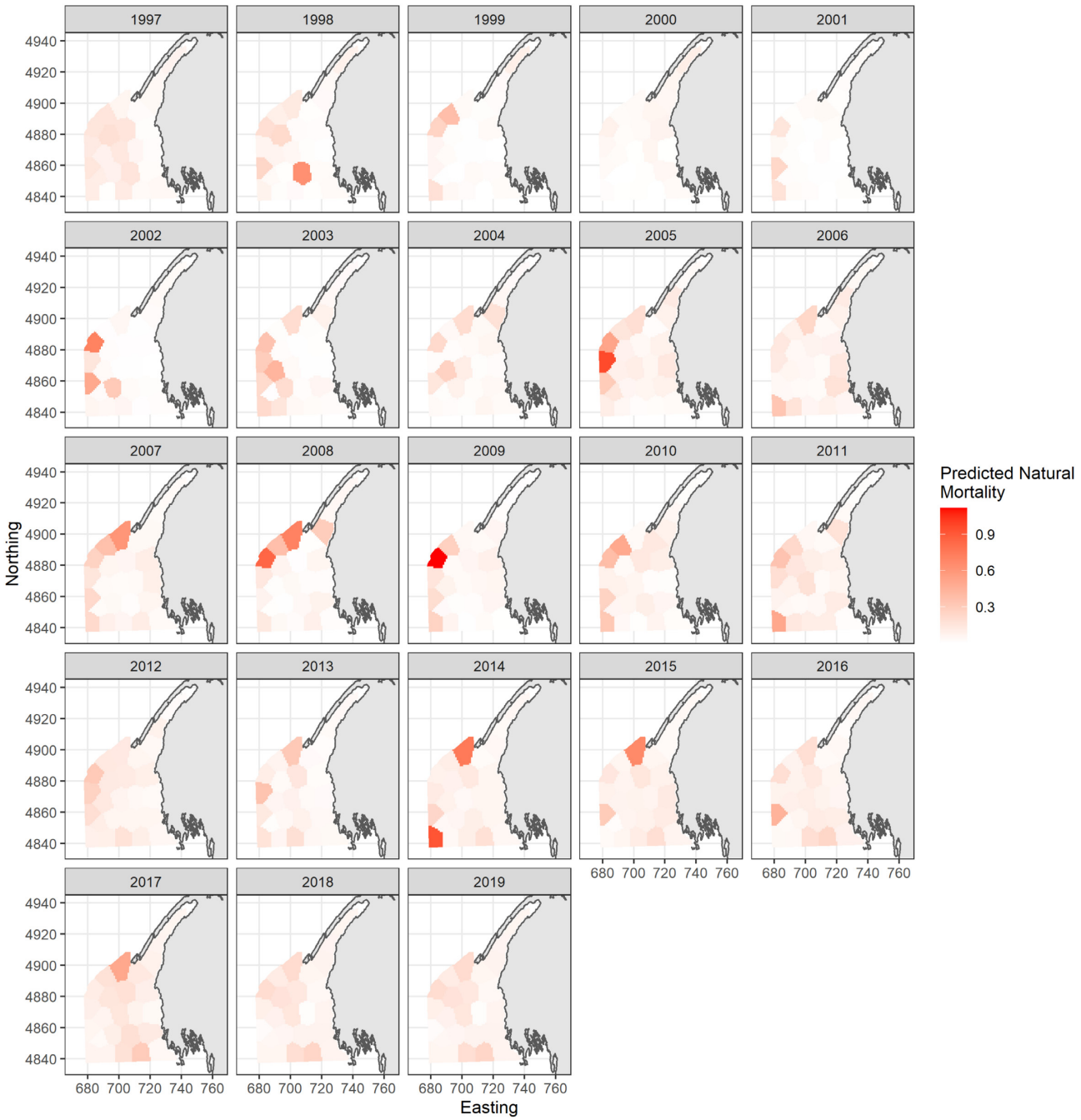

Figure 9. Predicted natural mortality $m_{s,t}$ at each knot between 1997 and 2018, with 1-year projections for 2019.

et al., 2019). SEBDAM is also able to provide a single synoptic biomass estimate for a region. All of the underlying processes are estimated with minimal bias, especially when a moderately informative prior is assumed for the catchability parameter. It is also able to project 1 year ahead with less associated uncertainty than its temporal predecessor (TLM) in a simplistic forecast setting.

Unusually large tows, characteristic of fisheries data, can unduly influence predicted population patterns and stock indices (Chen *et al.*, 2000; Hinrichsen, 2001). Although these tows contain real information, non-spatial methods tend to give them undue weight. In the SPA 3 time series, there are large spikes in biomass, recruitment and natural mortality. However, a closer inspection reveals that these spikes are due to a few tows that are constrained to relatively isolated areas [see Supplementary Materials and Nasmith *et al.* (2016)]. Stratification approaches help reduce the impact of these tows on analyses (Smith, 1996; Kimura and Somerton, 2006), but the influence of such large rare events still persist. Desirably, this spatio-temporal approach accounts for both the local and overall impact of these tows by borrowing information from neighboring tows. That is, the impact of outlying tows is informed by their spatial extent rather than their magnitude (or that of a small cluster of outlying tows).

SEDBAM captures and predicts spatial population and productivity patterns without explicitly modelling the underlying causal

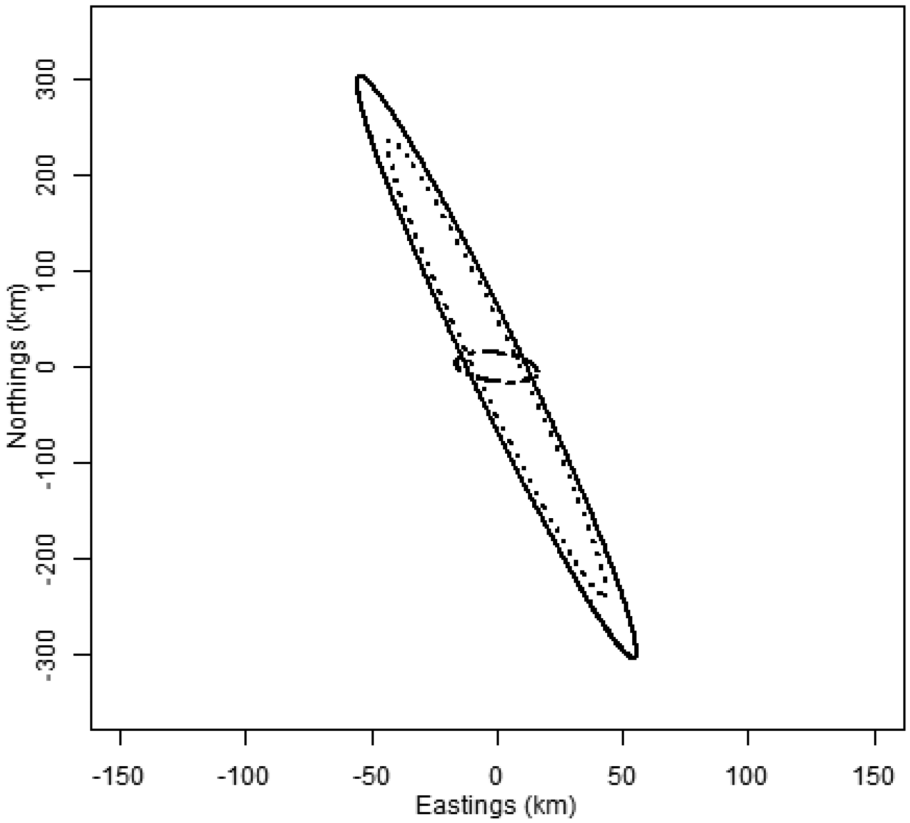

Figure 10. Decorrelation ranges in all directions for biomass (solid line), recruitment (dotted line), and natural mortality (dashed line).

mechanisms. By capturing the spatial information contained in the data, the latent impact of the environment on the population is modelled without explicit knowledge of the environmental factors driving these patterns (Besag, 1974; Legendre, 1993). Given that relationships between easily measured proxies for environmental drivers and population dynamics are known to change over time (Myers, 1998), the development of models which can track spatio-temporal changes in productivity patterns can help to provide deeper insights into the factors driving changes in productivity (Guan *et al.*, 2019). This incorporation of the environment without modelling the underlying mechanisms can therefore be seen as embracing an ecosystem approach to fisheries management (EAFM; Colloca *et al.*, 2013; Laugen *et al.*, 2014; Gullestad *et al.*, 2017; Bastardie *et al.*, 2021) and is part of the necessary work required to build up next-generation SAMs (Cadrin, 2020; Punt *et al.*, 2020).

Explicitly modelling key characteristics of a given stock as spatial processes has been identified as an essential feature of next-generation assessment models (Berger *et al.*, 2017; Punt *et al.*, 2020). Our approach improves on many of the challenges that need to be addressed to move in this direction, from the incorporation of spatial structure to the inclusion of a simulation framework (Berger *et al.*, 2017; Punt *et al.*, 2020). SEBDAM can explicitly model the spatial structure inside of a stock by tracking the population density at a data-driven resolution, and is able to incorporate spatial random effects using computationally efficient methods through the use of TMB. Furthermore, SEBDAM has a built-in simulation framework that allows for "self-tests" (Punt *et al.*, 2020) under various settings and can be combined with other methods to show patterns of biases that come from ignoring spatial structure (see Appendix A). While SEBDAM does not explicitly model the impact of specific environmental factors, its ability to capture spatio-temporal patterns in productivity can help us formulate hypotheses to explain the drivers of these patterns.

By combining the predicted population patterns with the estimated decorrelation ranges, we can make inferences about the causal mechanisms driving observed environmental patterns. In the case of SPA 3, there is a clear productivity gradient from east (higher productivity) to west (lower productivity) where all three processes follow the bathymetry and/or tidal flow in some way. This aligns with the depth profiles, major currents and tidal flows of the Bay of Fundy (Hannah *et al.*, 2001; Aretxabaleta *et al.*, 2008) that likely impact the growth and survival of scallops that have settled into the benthic environment (Shumway *et al.*, 1987; Smith and Rago, 2004). The habitat suitability for benthic species such as scallops is often related to bathymetry (Brown *et al.*, 2012), and it has been linked to increased productivity, increased fishing pressure (Brown *et al.*, 2012; Smith *et al.*, 2017), and to settlement success for juvenile scallops (Hart and Chute, 2004). Work has already gone into identifying and creating habitat suitability maps for sea scallops (Brown *et al.*, 2012) and while they have been used to develop precautionary approach reference points for the purpose of stock assessment (Smith and Sameoto, 2016; Smith *et al.*, 2017), these maps have not yet been used as direct inputs into the SAMs themselves. Using habitat information to incorporate suitability patterns promises to further improve these types of spatially-explicit models.

Our approach provides science advice for the entire management area as well as any subset of interest. It can be used to provide the information necessary for traditional forms of science advice, such

Figure 11. Predicted total biomass, total recruitment and mean natural mortality for SPA 3 from TLM (red) and SEBDAM (blue). Envelopes represent interpolated point-wise 95% confidence intervals.

as biomass reference points and removal reference points while also facilitating the development of novel indices that can be used to develop new types of science advice (Caddy and Mahon, 1995; Nasmith *et al.*, 2016; Shertzer *et al.*, 2010; Smith *et al.*, 2017) such as dynamic reference points (Berger, 2019) by capturing shifts in productivity or simply guide the development of spatial reference points (Reuchlin-Hugenholtz *et al.*, 2016). Entirely new management tools could also be developed, for example "hierarchical" reference points in which typical synoptic reference points for an entire stock could be retained (Caddy and Mahon, 1995; Shertzer *et al.*, 2010). These could then be used alongside more targeted reference points, which focus on management measures to protect particular spatial regions within the stock [similar to managing on spawning stock biomass within more productive regions such as examples in Pikitch *et al.* (2012)] or focusing on regions in which exploitation tends to be elevated (Nasmith *et al.*, 2016). Incorporating spatial information into traditional SAMs opens up the possibilities of developing new types of science advice that can help facilitate sustainable fisheries management goals.

The ability of our spatio-temporal approach to capture population changes with minimal bias represents an improvement over more traditional temporal approaches and brings to light the importance of including spatial structure. Embracing a spatio-temporal approach implicitly embraces an EAFM by incorporating the impact of unmodelled environmental processes while simultaneously informing reasonable hypotheses of what these processes might be. Further, "going spatial" enables the assessment models to be future proofed against shifts in productivity or fishing effort without requiring extensive work modifying survey strata and subsequent indices. This approach increases the amount of information available to fisheries managers, reduces the uncertainty around the traditional estimates of population size, and should subsequently increase the confidence in the scientific advice provided to managers and stakeholders, thereby reducing the inherent risk in fisheries management decision-making.

SUPPORTING INFORMATION

Supplementary material is available at the *ICESJMS* online version of the manuscript.

Data Availability Statement

The survey data underlying this article are available at https://github.com/RaphMcDo/SPA3-Case-Study. The landings data cannot be shared publicly as they are protected by privacy laws.

Acknowledgements

Research funding was provided by the Ocean Frontiers Institute, through an award from the Canada First Research Excellence Fund, and from a Nova Scotia Graduate Scholarship.

REFERENCES

Aeberhard, W. H., Flemming, J. M., and Nielsen, A. 2018. Review of state-space models for fisheries science. Annual Review of Statistics and Its Application, 5: 215–235.

Aretxabaleta, A. L., McGillicuddy, D. J., Smith, K. W., and Lynch, D. R. 2008. Model simulations of the Bay of Fundy Gyre: 1. Climatological results. Journal of Geophysical Research: Oceans, 113: 1–16.

Aubry, P., and Debouzie, D. 2000. Geostatistical estimation variance for the spatial mean in two-dimensional systematic sampling. Ecology, 81: 543–553.

Auger-Méthé, M., Albertsen, C. M., Jonsen, I. D., Derocher, A. E., Lidgard, D. C., Studholme, K. R., Bowen, W. D. *et al.*, 2017. Spatiotemporal modelling of marine movement data using Template Model Builder (TMB). Marine Ecology Progress Series, 565: 237–249.

Baranov, T. 1918. On the question of the biological basis of fisheries. Proceedings of the Institute of Ichthyology Investments, 1: 81–128.

Bastardie, F., Brown, E. J., Andonegi, E., Arthur, R., Beukhof, E., Depestele, J., Döring, R. *et al.* 2021. A review characterizing 25 ecosystem challenges to be addressed by an ecosystem approach to fisheries management in Europe. Frontiers in Marine Science, 7: 1241.

Berger, A. M. 2019. Character of temporal variability in stock productivity influences the utility of dynamic reference points. Fisheries Research, 217: 185–197.

Berger, A. M., Goethel, D. R., Lynch, P. D., Quinn, T., Mormede, S., McKenzie, J., and Dunn, A. 2017. Space oddity: the mission for spatial integration. Canadian Journal of Fisheries and Aquatic Sciences, 1716: 1–19.

Besag, J. 1974. Spatial interaction and the statistical analysis of lattice systems. Journal of Royal Statistical Society. Series B (Methodological), 36: 192–236.

Best, J. K., and Punt, A. E. 2020. Parameterizations for Bayesian state-space surplus production models. Fisheries Research, 222: 1–9.

Beverton, R. J. H., and Holt, S. J. 1957. On the Dynamics of Exploited Fish Populations. Ministry of Agriculture, Fisheries and Food, London, UK.

Brown, C. J., Sameoto, J. A., and Smith, S. J. 2012. Multiple methods, maps, and management applications: purpose made seafloor maps in support of ocean management. Journal of Sea Research, 72: 1–13.

Caddy, J. F. 1975. Spatial model for an exploited shellfish population, and its application to the Georges Bank scallop fishery. Journal of the Fisheries Research Board of Canada, 32: 1305–1328.

Caddy, J. F., and Mahon, R. 1995. Reference points for fisheries management. FAO Fisheries Technical Paper No. 347.

Cadigan, N. G., Wade, E., and Nielsen, A. 2017. A spatiotemporal model for snow crab (*Chionoecetes opilio*) stock size in the southern Gulf of St. Lawrence. Canadian Journal of Fisheries and Aquatic Sciences, 74: 1808–1820.

Cadrin, S. X. 2020. Defining spatial structure for fishery stock assessment. Fisheries Research, 221: 105397.

Cao, J., Thorson, J. T., Punt, A. E., and Szuwalski, C. 2019. A novel spatiotemporal stock assessment framework to better address fine-scale species distributions: development and simulation testing. Fish and Fisheries, 21: 350–367.

Carson, S., Shackell, N., and Mills Flemming, J. 2017. Local overfishing may be avoided by examining parameters of a spatio-temporal model. PLoS One, 12: 1–21.

Chen, Y., Breen, P. A., and Andrew, N. L. 2000. Impacts of outliers and mis-specification of priors on Bayesian fisheries-stock assessment. Canadian Journal of Fisheries and Aquatic Sciences, 57: 2293–2305.

Ciannelli, L., Fauchald, P., Chan, K. S., Agostini, V. N., and Dingsør, G. E. 2008. Spatial fisheries ecology: recent progress and future prospects. Journal of Marine Systems, 71: 223–236.

Colloca, F., Cardinale, M., Maynou, F., Giannoulaki, M., Scarcella, G., Jenko, K., Bellido, J. M. *et al.*, 2013. Rebuilding Mediterranean fisheries: a new paradigm for ecological sustainability. Fish and Fisheries, 14: 89–109.

Costello, C., Ovando, D., Hilborn, R., Gaines, S. D., Deschenes, O., and Lester, S. E. 2012. Status and solutions for the world's unassessed fisheries. Science, 338: 517–520.

Deriso, R. B. 1980. Harvesting strategies and parameter estimation for an age-structured model. Canadian Journal of Fisheries and Aquatic Sciences, 37: 268–282.

Eriksson, H., and Byrne, M. 2015. The sea cucumber fishery in Australia's Great Barrier Reef Marine Park follows global patterns of serial exploitation. Fish and Fisheries, 16: 329–341.

Froese, R. 2006. Cube law, condition factor and weight-length relationships: history, meta-analysis and recommendations. Journal of Applied Ichthyology, 22: 241–253.

Glass, A. 2017. Maritimes region inshore scallop assessment survey: detailed technical description. Technical Report. Canadian Technical Report of Fisheries and Aquatic Sciences 3231.

Greenlaw, M. E., Sameoto, J. A., Lawton, P., Wolff, N. H., Incze, L. S., Smith, S. J., and Drozdowski, A. 2010. A geodatabase of historial and contemporary oceanographic datasets for investigating the role of the physical environment in shaping patterns of seabed biodiversity in the Gulf of Maine. Technical Report. Fisheries and Oceans Canada.

Guan, L., Chen, Y., Wilson, J. A., Waring, T., Kerr, L. A., and Shan, X. 2019. The influence of spatially variable and connected recruitment on complex stock dynamics and its ecological and management implications. Canadian Journal of Fisheries and Aquatic Sciences, 76: 937–949.

Gullestad, P., Abotnes, A. M., Bakke, G., Skern-Mauritzen, M., Nedreaas, K., and Søvik, G. 2017. Towards ecosystem-based fisheries management in Norway – practical tools for keeping track of relevant issues and prioritising management efforts. Marine Policy, 77: 104–110.

Hannah, C. G., Shore, J. A., and Loder, J. W. 2001. Seasonal circulation on the Western and Central Scotian Shelf. Journal of Physical Oceanography, 31: 591–615.

Hart, D. R., and Chute, a. S. 2004. Essential fish habitat source document. Sea scallop, *Placopecten magellanicus*, life history and habitat characteristics. Technical Report. NOAA Technical Memorandum NMFS-NE: 189.

Hilborn, R. 1992. Current and future trends in fisheries stock assessment and management. South African Journal of Marine Science, 12: 975–988.

Hinrichsen, R. A. 2001. The importance of influence diagnostics: examples from Snake River chinook salmon spawner-recruit models. Canadian Journal of Fisheries and Aquatic Sciences, 58: 551–559.

Hutchings, J. 1996. Spatial and temporal variation in the density of northern cod and a review of hypotheses for the stock's collapse. Canadian Journal of Fisheries and Aquatic Sciences, 53: 943–962.

Hutchings, J. A., and Myers, R. A. 1994. What can be learned from the collapse of a renewable resource? Atlantic cod, *Gadus morhua*, of Newfoundland and Labrador. Canadian Journal of Fisheries and Aquatic Sciences, 51: 2126–2146.

Illian, J. B., Sørbye, S. H., and Rue, H. 2012. A toolbox for fitting complex spatial point process models using integrated nested Laplace approximation (INLA). Annals of Applied Statistics, 6: 1499–1530.

Kimura, D. K., and Somerton, D. A. 2006. Review of statistical aspects of survey sampling for marine fisheries. Reviews in Fisheries Science, 14: 245–283.

Kinas, P. G. 1996. Bayesian fishery stock assessment and decision making using adaptive importance sampling. Canadian Journal of Fisheries and Aquatic Sciences, 53: 414–423.

Kristensen, K., Nielsen, A., Berg, C. W., Skaug, H., and Bell, B. 2016. TMB: automatic differentiation and Laplace approximation. Journal of Statistical Software, 70: 1–21.

Laugen, A. T., Engelhard, G. H., Whitlock, R., Arlinghaus, R., Dankel, D. J., Dunlop, E. S., Eikeset, A. M. *et al.*, 2014. Evolutionary impact assessment: accounting for evolutionary consequences of fishing in an ecosystem approach to fisheries management. Fish and Fisheries, 15: 65–96.

Legendre, P. 1993. Spatial autocorrelation: trouble or new paradigm? Ecology, 74: 1659–1673.

Lindgren, F., and Rue, H. 2011. An explicit link between Gaussian fields and Gaussian Markov random fields: the stochastic partial differential equation approach. Journal of the Royal Statistical Society: Series B, 73: 423–498.

Lindgren, F. K. 2012. Continuous domain spatial models in R-INLA. The ISBA Bulletin, 19: 1–8.

McDonald, R. R., Keith, D. M., Sameoto, J. A., Hutchings, J. A., and Mills Flemming, J. 2021. Incorporating intra-annual variability in fisheries abundance data to better capture population dynamics. Fisheries Research, in press.

Miller, T. J., Hart, D. R., Hopkins, K., Vine, N. H., Taylor, R., York, A. D., and Gallager, S. M. 2019. Estimation of the capture efficiency and abundance of atlantic sea scallops (*Placopecten magellanicus*) from paired photographic–dredge tows using hierarchical models. Canadian Journal of Fisheries and Aquatic Sciences, 76: 847–855.

Myers, R. A. 1998. When do environment-recruitment correlations work? Reviews in Fish Biology and Fisheries, 8: 285–305.

Myers, R. A., Hutchings, J. A., and Barrowman, N. J. 1996. Hypotheses for the decline of cod in the North Atlantic. Marine Ecology Progress Series, 138: 293–308.

Nasmith, L., Sameoto, J. A., and Glass, A. 2016. Scallop production areas in the Bay of Fundy: stock status for 2015 and forecast for 2016. Technical Report 2016/021. Fisheries and Oceans Canada.

Pedersen, M. W., and Berg, C. W. 2017. A stochastic surplus production model in continuous time. Fish and Fisheries, 18: 226–243.

Pikitch, E., Boersma, P., Boyd, I., Conover, D., Cury, P., Essington, T., Heppell, S. *et al.* 2012. Little fish, big impact: managing a crucial link in ocean food webs. Technical Report. Lenfest Forage Fish Task Force.

Punt, A. E., Dunn, A., Elvarsson, B. ó., Hampton, J., Hoyle, S. D., Maunder, M. N., Methot, R. D. *et al.*, 2020. Essential features of the next-generation integrated fisheries stock assessment package: a perspective. Fisheries Research, 229: 105617.

Rawson, K., and Hoagland, P. 2019. Sea cucumbers in a pickle: the economic geography of the serial exploitation of sea cucumbers. Ecology and Society, 24: 35.

Reuchlin-Hugenholtz, E., Shackell, N. L., and Hutchings, J. A. 2015. The potential for spatial distribution indices to signal thresholds in marine fish biomass. PLoS One, 10: 1–22.

Reuchlin-Hugenholtz, E., Shackell, N. L., and Hutchings, J. A. 2016. Spatial reference points for groundfish. ICES Journal of Marine Science, 73: 2468–2478.

Schnute, J. 1985. A general theory for analysis of catch and effort data. Canadian Journal of Fisheries and Aquatic Sciences, 42: 414–429.

Shaw, J., Todd, B. J., and Li, M. Z. 2014. Geologic insights from multibeam bathymetry and seascape maps of the Bay of Fundy, Canada. Continental Shelf Research, 83: 53–63.

Shaw, J., Todd, B. J., Li, M. Z., and Wu, Y. 2012. Anatomy of the tidal scour system at Minas Passage, Bay of Fundy, Canada. Marine Geology, 323–325: 123–134.

Shertzer, K. W., Prager, M. H., and Williams, E. H. 2010. Probabilistic approaches to setting acceptable biological catch and annual catch targets for multiple years: reconciling methodology with national standards guidelines. Marine and Coastal Fisheries, 2: 451–458.

Shumway, S., Selvin, R., and Schick, D. 1987. Food resources related to habitat in the scallop, *Placopecten magellanicus* (Gmelin 1791): a qualitative study. Journal of Shellfish Research, 6: 89–95.

Smith, S. J. 1996. Analysis of data from bottom trawl surveys. NAFO Scientific Council Studies, 28: 25–53.

Smith, S. J., and Hubley, B. 2014. Impact of survey design changes on stock assessment advice: sea scallops. ICES Journal of Marine Science, 72: 82–92.

Smith, S. J., Hubley, B., Nasmith, L., Sameoto, J. A., Bourdages, H., and Glass, A. 2012. Scallop production areas in the Bay of Fundy: stock status for 2011 and forecast for 2012. Research Document 2016/021. Fisheries and Oceans Canada.

Smith, S. J., and Lundy, M. J. 2002. Scallop production area 4 in the Bay of Fundy: stock status and forecast. Research Document 2002/018, Fisheries and Oceans Canada.

Smith, S. J., and Rago, P. 2004. Biological reference points for sea scallops (*Placopecten magellanicus*): the benefits and costs of being nearly sessile. Canadian Journal of Fisheries and Aquatic Sciences, 61: 1338–1354.

Smith, S. J., and Sameoto, J. A. 2016. Incorporating habitat suitability into productivity estimates for sea scallops in scallop fishing area 29 west. Research Document 2016/107. Fisheries and Oceans Canada.

Smith, S. J., Sameoto, J. A., and Brown, C. J. 2017. Setting biological reference points for sea scallops (*Placopecten magellanicus*) allowing

for the spatial distribution of productivity and fishing effort. Canadian Journal of Fisheries and Aquatic Sciences, 74: 650–667.

Stock, B. C., Ward, E. J., Eguchi, T., Jannot, J. E., Thorson, J. T., Feist, B. E., and Semmens, B. X. 2020. Comparing predictions of fisheries bycatch using multiple spatiotemporal species distribution model frameworks. Canadian Journal of Fisheries and Aquatic Sciences, 77: 146–163.

Thorson, J. T., Adams, G., and Holsman, K. 2019. Spatio-temporal models of intermediate complexity for ecosystem assessments: a new tool for spatial fisheries management. Fish and Fisheries, 20: 1083–1099.

Thorson, J. T., and Barnett, L. A. 2017. Comparing estimates of abundance trends and distribution shifts using single- and multispecies models of fishes and biogenic habitat. ICES Journal of Marine Science, 74: 1311–1321.

Thorson, J. T., Ianelli, J. N., Munch, S. B., Ono, K., Spencer, P. D., and Vinbrooke, R. 2015a. Spatial delay-difference models for estimating spatiotemporal variation in juvenile production and population abundance. Canadian Journal of Fisheries and Aquatic Sciences, 72: 1897–1915.

Thorson, J. T., Shelton, A. O., Ward, E. J., and Skaug, H. J. 2015b. Geostatistical delta-generalized linear mixed models improve precision for estimated abundance indices for West Coast groundfishes. ICES Journal of Marine Science, 72: 1297–1310.

Venables, W. N., and Dichmont, C. M. 2004. GLMs, GAMs and GLMMs: an overview of theory for applications in fisheries research. Fisheries Research, 70: 319–337.

Yin, Y., Aeberhard, W. H., Smith, S. J., and Mills Flemming, J. 2019. Identifiable state-space models: a case study of the Bay of Fundy sea scallop fishery. Canadian Journal of Statistics, 47: 27–45.

Handling Editor: Sam Subbey